

Published in final edited form as:

Invest Ophthalmol Vis Sci. 2005 November ; 46(11): 4320–4327.

A Critical Role of CaBP4 in the Cone Synapse

Tadao Maeda¹, Janis Lem², Krzysztof Palczewski^{1,3,4}, and Françoise Haeseleer¹

¹ From the Departments of Ophthalmology,

³ Pharmacology, and

⁴ Chemistry, University of Washington, Seattle, Washington; and the

² Departments of Ophthalmology and Molecular Cardiology, Tufts–New England Med Center, Boston, Massachusetts.

Abstract

Purpose—CaBP4, a photoreceptor-specific protein of the rods and cones, is essential for the development and maintenance of the mouse photoreceptor synapse. In this study, double CaBP4/rod α -transducin knockout (*Cabp4*^{-/-}*Gnat1*^{-/-}) mice lacking the rod-mediated component of electrophysiologic responses were generated and analyzed to investigate the role of CaBP4 in cones.

Methods—The retinal morphology and physiologic function of 2-month-old *Cabp4*^{-/-}*Gnat1*^{-/-} mice were analyzed using immunocytochemistry, electron microscopy, and single-flash and flicker electroretinography (ERG).

Results—The thickness of the outer plexiform layer and the number of photoreceptor terminals in *Cabp4*^{-/-}*Gnat1*^{-/-} mice were reduced to levels similar to those of *Cabp4*^{-/-} mice. Single-flash and flicker ERG showed that the amplitude and sensitivity of the b-wave in the *Cabp4*^{-/-}*Gnat1*^{-/-} mice were severely attenuated compared with those in wild-type and *Gnat1*^{-/-} mice.

Conclusions—Results indicate that the cone synaptic function in *Cabp4*^{-/-}*Gnat1*^{-/-} mice was severely disrupted, whereas the morphologic defects observed in *Cabp4*^{-/-}*Gnat1*^{-/-} mice were similar to those of single *Cabp4*^{-/-} knockout mice. This and a previous study reveal that CaBP4 is critical for signal transmission from rods and cones to second-order neurons.

CaBP4, a photoreceptor-specific protein originally isolated in our laboratory from retina cDNAs,^{1,2} is a member of a subfamily of neuronal Ca²⁺-binding proteins (CaBPs), which display a high similarity to calmodulin (CaM).^{1–4} CaBP4, CaBP2, and CaBP5 are retina-specific Ca²⁺-binding proteins. CaBP1, CaBP2, and CaBP5 have been shown to target proteins known to be modulated by calmodulin, such as G protein-coupled receptor kinase 2, calmodulin kinase II, and calcineurin.^{1,5} In vitro, CaBP1 also modulates the L-type and P/Q-type voltage-gated Ca²⁺ channels and the inositol triphosphate (IP₃) receptor.^{6–8}

In the mouse eye, CaBP4 is localized at the photoreceptor synaptic terminals in rods and cones. CaBP4 is essential for the development and maintenance of the photoreceptor synapse, likely through functional modulation of the photoreceptor Ca²⁺ channels, α 1F L-type voltage-dependent calcium channels (Ca_v1.4), and neurotransmitter release.² Photoreceptor synapses in CaBP4-deficient (*Cabp4*^{-/-}) mice are severely disrupted anatomically and functionally. ERG measurements and single-cell recordings show a disruption in the transmission from

Corresponding author: Françoise Haeseleer, Department of Ophthalmology, University of Washington, Box 356485, Seattle, WA 98195; fanfan@u.washington.edu..

Supported by National Institutes of Health Grants EY014561 (FH), EY12008 (JL), and EY09339 (KP); a grant from the E.K. Bishop Foundation; and Vision Core Grant EY01730.

Disclosure: T. Maeda, None; J. Lem, None; K. Palczewski, None; F. Haeseleer, None

photoreceptors to bipolar cells in *Cabp4*^{-/-} mice, whereas rod phototransduction is only modestly affected.

Mutations in the *CACNA1F* gene (Ca_v1.4 gene) are responsible for incomplete congenital stationary night blindness (CSNB2).⁹ Interestingly, the phenotypes of these patients and of mice deficient for the β2 subunit of the Ca_v1.4 channel¹⁰ are similar to those of *Cabp4*^{-/-} mice. In a previous study, we demonstrated that the signal transfer from rods to rod bipolar cells is altered in *Cabp4*^{-/-} mice by measuring light responses of rod bipolar cells.² Ca_v1.4 channel expression has been clearly shown in rods but not yet in cones. Thus cone function response cannot be either clearly inferred from our initial ERG experiments or ascribed to CaBP4 – Ca_v1.4 channel interaction. Furthermore, 30-Hz flicker ERG responses of CSNB2 patients carrying *CACNA1F* gene mutations suggest markedly depressed cone functions,¹¹ though these patients have normal color vision.¹²

It is important to evaluate the function of CaBP4 in cones to understand its role in the development and maintenance of the photoreceptor synapse between cone and bipolar cells and its contribution to the cone phenotype of CSNB2 patients. For this purpose, mice lacking functional rod transducin (*Gnat1*^{-/-}) were crossbred with *Cabp4*^{-/-} mice to generate *Cabp4*^{-/-}*Gnat1*^{-/-} mice. The *Gnat1*^{-/-} mouse is a useful model to evaluate pure cone function under all light conditions and has been characterized extensively by Calvert et al.¹¹ We have analyzed and compared the retinal morphology and light responses of wild-type, CaBP4, rod α-transducin, and CaBP4/rod α-transducin knockout mice with single-flash and flicker ERG to evaluate the cone function of each genotype more precisely.

MATERIALS AND METHODS

Generation and Genotyping of *Cabp4*^{-/-} *Gnat1*^{-/-} Knockout Mice

The mice were housed in the Department of Comparative Medicine at the University of Washington and were treated according to the ARVO Statement for the Use of Animals in Ophthalmic and Vision Research. The double-knockout mice were generated by breeding *Cabp4*^{-/-} mice² and *Gnat1*^{-/-} mice.¹¹ The genotype of the mutant mice was confirmed by PCR. To identify the wild-type allele, the primer pair FH589 (5'-GTACACATGTAGATGCAGGAG-3', hybridizing in intron 4 of mouse *Gnat1*) and FH588 (5'-CACCAGCACCATGTCGTAAG-3', located in exon 6 of mouse *Gnat1*) was used to give a PCR product of ~500 bp. The targeted CaBP4 allele was identified with primers K183 (5'-CTTGCGAATATCATGGTGG-3', located in the neo-cassette) and FH588 and gave a PCR product of approximately 600 bp. The PCRs were cycled at 94°C for 5 minutes, followed by 35 cycles at 94°C for 30 seconds, 60°C for 30 seconds, and 72°C for 1.5 minutes, followed by a final extension at 72°C for 7 minutes. *Cabp4*^{-/-}, *Gnat1*^{-/-}, and *Cabp4*^{-/-}*Gnat1*^{-/-} mice were in a mixed C57BL/6, 129SvEv, and BALB/c background. The wild-type mice were C57Bl/6.

Antibodies

Monoclonal mouse anti-PSD95 (clone K28/43) was purchased from Upstate Biotechnology (Lake Placid, NY.). Mouse monoclonal anti-Bassoon was purchased from Stressgen (Victoria, BC, Canada). Rabbit anti-protein kinase C α- (sc-208) and anti-rod α-transducin (sc-389) were purchased from Santa Cruz Biotechnology, Inc. (Santa Cruz, CA). Labeled peanut agglutinin (PNA) and conjugated goat anti-mouse IgG were purchased from Molecular Probes, Inc. (Alexa 488; Eugene, OR). Cy3-conjugated goat anti-rabbit IgG and anti-mouse IgG were purchased from Jackson ImmunoResearch Laboratories, Inc. (West Grove, PA). The generation of rabbit polyclonal anti-CaBP4 was described previously.²

Immunocytochemistry

Mouse eyecups were fixed in 4% paraformaldehyde in 0.1 M phosphate buffer (PB; 100 mM sodium phosphate, pH 7.4) for 4 hours. After fixation, the tissues were infiltrated with graded sucrose solutions (5%, 10%, 15%, and 20% sucrose in PB), and then embedded in 33% OCT compound (Miles, Elkhart, IN) diluted with 20% sucrose in PB. Eye tissues were cut in 10- μ m sections. To block non-specific labeling, retinal sections were incubated with 3% normal goat serum in PBST buffer (136 mM NaCl, 11.4 mM sodium phosphate, 0.1% Triton X-100, pH 7.4) for 20 minutes at room temperature. Sections were incubated overnight at 4°C in diluted primary antibodies. Sections were washed with PBST. For single staining, sections were incubated with Cy3-conjugated goat anti-rabbit IgG. For double staining, a mixture of Cy3-conjugated goat anti-rabbit IgG and conjugated goat anti-mouse IgG (Alexa 488; Molecular Probes) was reacted with sections. For double staining including PNA, sections were incubated with PNA and Cy3-conjugated goat anti-rabbit IgG (Alexa 488; Molecular Probes). Sections were stained with Hoechst 33342 dye (Molecular Probes) to reveal the nuclei. Then, sections were rinsed in PBST and mounted with antifade reagent (Prolong; Molecular Probes) to retard photo-bleaching. For experiments using retinal whole-mounts, the retinas were dissected as described previously.¹² The retinas were incubated with 5% normal goat serum in PBST buffer (136 mM NaCl, 11.4 mM sodium phosphate, 0.1% Triton X-100, pH 7.4) overnight at 4°C and then again overnight at 4°C with anti-bassoon antibody (1:500). After three washes for 15 minutes in PBST, Cy-3-conjugated goat anti-mouse (1:100) or PNA (1:50; Alexa 488; Molecular Probes) was added to the retina overnight at 4°C. Retinal whole-mounts were mounted with the photoreceptor side up.

Sections were analyzed under a confocal microscope (Zeiss LSM510; Carl Zeiss, New York, NY.). Immunofluorescent images were obtained with a 40 \times /1.3 NA objective lens (Plan-Neofluar; Carl Zeiss). Projections of confocal images were made using LSM510 software 3.0 (Carl Zeiss).

Transmission Electron Microscopy

Mouse eyecups were primarily fixed by immersion in 2.5% glutaraldehyde, 1.6% paraformaldehyde in pH 7.4, 0.08 M piperazine diethane-sulfonic acid (PIPES) buffer containing 2% sucrose, initially at room temperature for approximately 1 hour, then at 4°C for the remainder of a 24-hour period. The eyecups were then washed with pH 7.35, 0.13 M phosphate buffer, and secondarily fixed with 1% OsO₄ in pH 7.4, 0.1 M phosphate buffer for 1 hour at room temperature. After another wash with 0.13 M phosphate buffer, the eyecups were dehydrated through a methanol series and transitioned to epoxy embedding medium with propylene oxide. The eyecups were infiltrated (Eponate 812; Ted Pella, Inc., Redding, CA) and embedded for sectioning in Eponate 812 by hardening at 70°C for 24 hours before ultramicrotomy. Ultrathin sections (60–70 nm) were cut with a diamond knife and mounted on 50-mesh grids coated with a film (Pioloform; Ted Pella). The sections were then stained with aqueous-saturated uranium acetate and Reynold's formula lead citrate before survey and micrography (CM10 electron microscope; Philips, Eindhoven, The Netherlands). A montage of individual images was created in Adobe Photoshop. Photoreceptor terminals and synaptic ribbons were counted from working prints of sections obtained from 3 eyes. Sections were analyzed from end to end.

Electroretinograms

Before recording, mice were dark adapted overnight. Under safety light, mice were anesthetized by intraperitoneal injection using 20 μ L/g body weight of 6 mg/mL ketamine and 0.44 mg/mL xylazine diluted in 10 mM sodium phosphate (pH 7.2) containing 100 mM NaCl. Pupils were dilated with 1% tropicamide. A contact lens electrode was placed on the eye, and a reference electrode and a ground electrode were placed in the ear and on the tail.

Electroretinograms were recorded with the universal testing and electrophysiologic system (UTAS E-3000; LKC Technologies, Inc., Gaithersburg, MD). Light intensity was calibrated by the manufacturer and was computer controlled. Mice were placed in a Ganzfeld chamber, and scotopic and photopic responses to flash stimuli were obtained from both eyes simultaneously.

Single-Flash Recording—Flash stimuli had a range of intensities (-3.7 to $2.8 \log \text{cd} \cdot \text{s} \cdot \text{m}^{-2}$), and white light flash duration was adjusted according to intensity ($20 \mu\text{s}$ – 1ms). Three to five recordings were made at >10 -second intervals, and for higher intensity, intervals were 10 minutes long or as indicated. There were no significant differences between the first and the fifth flashes. Photopic responses were examined after bleaching at $1.4 \log \text{cd} \cdot \text{m}^{-2}$ for 15 minutes. Four to eight 2-month-old animals were typically used for the recording of each point in all conditions.

Flicker-Flash Recording—The recordings were performed following the same procedure as for single-flash recording. Flicker stimuli had a range of intensities (-3.7 to $1.4 \log \text{cd} \cdot \text{s} \cdot \text{m}^{-2}$) with various frequencies (5 – 30Hz). Statistical analysis was carried out using one-way ANOVA.

RESULTS

Morphologic Changes of the Retina

The morphology and the expression of relevant proteins were first analyzed in 2-month-old mice with antibodies directed against CaBP4 and rod α -transducin proteins. As expected, no CaBP4 proteins were detected in the *Cabp4*^{-/-} and *Cabp4*^{-/-}*Gnat1*^{-/-} retinas, and no α -transducin proteins were observed in the *Gnat1*^{-/-} and *Cabp4*^{-/-}*Gnat1*^{-/-} mice (Fig. 1). The localization of CaBP4 in *Gnat1*^{-/-} and transducin in *Cabp4*^{-/-} was similar to that in the wild-type mice. The thickness of all nuclear layers except the outer plexiform layer was unaltered in all knockout mice compared with the wild-type mice. To determine whether the cones were preserved in all knockout mice, we labeled the cones with fluorescein-labeled PNA. There was no difference in either the pattern of PNA staining or the number of cone photoreceptors in wild-type and all knockout mice (Figs. 2A–D). The inset points out the localization of CaBP4 in cones also labeled with PNA (Fig. 2A). CaBP4 staining was observed at the cone synaptic pedicles alongside the PNA-labeled synaptic membranes. CaBP4 staining was also observed in the rod spherules not labeled with PNA. To analyze the morphology of the synapse, an antibody against the pre-synaptic protein PSD95 was used to label the photoreceptor presynapse. The anti-protein kinase C alpha (PKC α) antibody was used to visualize the neuronal processes of rod bipolar cells. *Gnat1*^{-/-} and wild-type mice showed comparable pericellular staining with anti-PKC α and developed dendrites (Figs. 2E, 2G). Inflated photoreceptor synaptic terminals were observed with anti-PSD95 in *Gnat1*^{-/-} and wild-type mice. Photoreceptor terminals were condensed in *Cabp4*^{-/-} and *Cabp4*^{-/-}*Gnat1*^{-/-} mice, and the dendrites of their rod bipolar cells were short and underdeveloped (Figs. 2F, 2H) compared with those of *Gnat1*^{-/-} and wild-type mice.

To investigate whether there was any regional deficit of the photoreceptor population, PNA labeling was carried out with whole-mount retina. No difference in the density of cones was observed among the four quadrants of the retina in 2-month-old mice (Fig. 3A). No significant difference in the number of cones labeled with PNA was observed in knockout mice compared with wild-type mice. Labeling with an anti-bassoon antibody was carried out with whole-mount retina to analyze the morphologic changes of the presynaptic ribbons in rod spherules and cone pedicles across the mouse retina. Horseshoe-shaped structures representing the bassoon-labeled ribbons were observed in wild-type and *Gnat1*^{-/-} mice, but mostly punctate staining

was observed in *Cabp4*^{-/-} and *Cabp4*^{-/-} *Gnat1*^{-/-} mice (Fig. 3B). Results similar to those for the temporal retina (Fig. 3B) were observed in the four quadrants of the retina (data not shown). PNA labeling of the cone pedicles in the outer plexiform layer was also analyzed with retinal whole-mounts. In wild-type and *Gnat1*^{-/-} mice, the PNA-labeled cone pedicles are well defined and round, but the cone pedicles of *Cabp4*^{-/-} and *Cabp4*^{-/-} *Gnat1*^{-/-} mice are more disorganized and appear spread out in a diamond-shaped structure (Fig. 3B).

Ultrastructural Analysis of Photoreceptors Using Transmission Electron Microscopy

The outer plexiform layer showed comparable ultrastructural changes in *Cabp4*^{-/-} and *Cabp4*^{-/-} *Gnat1*^{-/-} mice (Figs. 4A–D, 4I–L). The photoreceptor terminals were condensed and less numerous than those of wild-type and *Gnat1*^{-/-} mice. Quantitative analysis of electron micrographs showed that the number of photoreceptor terminals is approximately 47% lower in *Cabp4*^{-/-} *Gnat1*^{-/-} (mean ± SD, 186 ± 39 photoreceptor terminals; *t*-test; *P* < 0.01; *n* = 3 eyes), approximately 40% lower in *Cabp4*^{-/-} (206 ± 57 photoreceptor terminals; *P* > 0.01; *n* = 3 eyes), and approximately 15% lower in *Gnat1*^{-/-} (296 ± 3 photoreceptor terminals; *P* > 0.05; *n* = 3 eyes) compared with wild-type mice (348 ± 39 photoreceptor terminals; *n* = 3 eyes). We also observed a reduction in the number of synaptic ribbons in the outer plexiform layer of *Cabp4*^{-/-} and *Cabp4*^{-/-} *Gnat1*^{-/-} of approximately 52% ± 10% (*P* < 0.001; *n* = 3 eyes) in comparison with that observed in wild-type mice.

The outer segments of knockout mice appeared normal compared with those of wild-type mice (i.e., parallel piles of disks extended from the inner segment to the retinal pigment epithelium (RPE) (Figs. 4A–H). The outer segments of *Cabp4*^{-/-} and *Cabp4*^{-/-} *Gnat1*^{-/-} were shorter by approximately 10% than those of the wild-type mice. Rods with outer segments shortened by malfunction or insufficiency of specific proteins are at risk.¹³ Changes in intermediate filament (glial fibrillary acidic protein [GFAP]) expression appear to be the earliest evidence of Müller cell responses to retinal degeneration. Therefore, we have compared the expression of GFAP in single- and double-knockout mice with those of wild-type mice. In wild-type and *Gnat1*^{-/-} mice, GFAP labeling was observed in astrocytes. In *Cabp4*^{-/-} and *Cabp4*^{-/-} *Gnat1*^{-/-} mice, GFAP labeling was observed mostly in astrocytes, but some staining was also observed in Müller cells (data not shown).

Analysis of Cone Function Using Electroretinogram Recordings

Electroretinograms of wild-type, *Cabp4*^{-/-}, *Gnat1*^{-/-}, and *Cabp4*^{-/-} *Gnat1*^{-/-} mice were recorded under scotopic and photopic conditions.

Scotopic Conditions—As expected from previous studies, no a-wave originating from rods was detected in 2-month-old *Gnat1*^{-/-} mice.¹⁴ Their b-wave resulting from cone-mediated responses showed reduced amplitude and was only detectable from $-1.0 \log \text{cd} \cdot \text{s} \cdot \text{m}^{-2}$ (Figs. 5A, 5B). In *Cabp4*^{-/-} mice, the amplitude of the a-wave was half the amplitude of that of wild-type mice, and the b-wave was even more severely affected (Figs. 5A, 5B). Both waves became detectable at intensities higher than $-2.0 \log \text{cd} \cdot \text{s} \cdot \text{m}^{-2}$. In the *Cabp4*^{-/-} *Gnat1*^{-/-} double-knockout mice, the a-wave and b-wave were almost absent, suggesting that there were no rod- and almost no cone-driven responses in scotopic conditions. These data also suggested that the b-wave observed in *Cabp4*^{-/-} mice under these conditions originated mostly from rod responses.

Photopic Conditions—Under photopic conditions, the sensitivity of the cones of single- and double-knockout mice was reduced compared with that of the wild type, and responses were not detected below $-1.0 \log \text{cd} \cdot \text{s} \cdot \text{m}^{-2}$ (Figs. 5C, 5D). The a-wave amplitude of *Cabp4*^{-/-} mice was reduced to half that of the wild-type in scotopic conditions; thus, the cone photoresponses were only modestly affected in single- and in double-knockout mice.

Amplitude and sensitivity of the b-wave of *Cabp4*^{-/-} and *Cabp4*^{-/-} *Gnat1*^{-/-} mice were greatly reduced (Figs. 5C, 5D). The b-wave amplitudes of *Cabp4*^{-/-} and *Cabp4*^{-/-} *Gnat1*^{-/-} mice reached a plateau level earlier than did those of wild-type mice, whereas the a-wave amplitudes increased with the stimulus intensities regardless of genetic background. Although similar, the b-wave response curves of the *Cabp4*^{-/-} *Gnat1*^{-/-} double knockout were lower than those of *Cabp4*^{-/-} mice, suggesting that some residual rod-driven responses were still detectable under these photopic conditions in *Cabp4*^{-/-} mice.

Flicker ERG—Flicker ERG to stimuli varying in temporal frequency and intensity was recorded to investigate cone responses. Pure cone responses are best characterized at 20 Hz¹⁵ or are dominantly observed at high-intensity 10-Hz stimulation in scotopic conditions.¹⁶ In scotopic conditions at 10 Hz, the sensitivity and amplitude of the flicker ERG were reduced significantly for all knockout mice compared with wild-type mice. Flicker ERG amplitudes of *Cabp4*^{-/-} and *Cabp4*^{-/-} *Gnat1*^{-/-} mice were significantly less than those of *Gnat1*^{-/-} mice. At a frequency of 20 Hz, a severe reduction in the amplitude of flicker ERG was observed for *Cabp4*^{-/-} and *Cabp4*^{-/-} *Gnat1*^{-/-} mice (Fig. 6). Surprisingly, the amplitude of *Gnat1*^{-/-} was also affected, though less than in the other knockout mice. Under photopic conditions, the sensitivity of the flicker ERG was similar for all mice. However, the amplitude of the flicker ERG was severely reduced at higher intensities (at > 0.6 log cd · s · m⁻²) for all knockout mice, though the reduction in *Gnat1*^{-/-} was again less severe. Together, these data demonstrate that the responses of cones and rods in CaBP4-deficient mice are significantly affected or absent in comparison with wild-type mice.

DISCUSSION

In this study, we have analyzed cone visual functions without interference from rod responses. This experimental design has allowed us to demonstrate that CaBP4 is crucial for synaptic transmission from cone photoreceptors to second-order neurons. To evaluate pure cone function, it is essential to block rod responses. Cone-mediated light responses can be isolated using rod-saturating conditions or flicker ERG at high frequency. However, residual rod responses might still be detected in photopic responses,¹⁵ and the use of a rod-saturating background might also affect cone responses. The drawback of flicker ERG in mice is the low signal-to-noise ratio at frequencies that are thought to be greater than rod temporal resolution.¹⁷ To characterize cone responses under photopic and scotopic conditions, we used knockout mice that have no functional rods. Diverse knockout models of rod dysfunction have been developed, including rhodopsin-deficient mice and rod α -transducin-deficient mice.^{11,18,19} The advantage of the rod α -transducin-deficient model over the rhodopsin-deficient mice is that the structure of rods is normal for the first 3 months, whereas that of rhodopsin-deficient mice degenerates rapidly.^{18,19}

In this study, to investigate the role of CaBP4 for cone vision, we crossbred *Cabp4*^{-/-} with *Gnat1*^{-/-} mice. These *Cabp4*^{-/-} *Gnat1*^{-/-} double-knockout mice allowed us to study the effect of CaBP4-deficiency without interference from rod-mediated responses. No detectable changes in retinal morphology between double-knockout mice and single-knockout mice were observed, and the cones were as well preserved in double-knockout mice as in single-knockout mice. These results indicate that the absence of photoexcitation in rods does not affect the CaBP4-deficient phenotype morphologically, confirming the suitability of this model to study the effect of CaBP4 deficiency on cone signaling function. These observations are in accordance with other findings that demonstrate that the absence of functional cones and rods does not affect the structural development of the photoreceptor synapses after eye opening.²⁰ Synaptic contacts between photoreceptor terminals, horizontal cell processes, and bipolar cell dendrites were also reported to be relatively normal in double cone cyclic nucleotide-gated cation channel /rhodopsin knockout mice up to postnatal week 4.²⁰

The absence of morphologic changes between these *Cabp4*^{-/-} and *Cabp4*^{-/-} *Gnat1*^{-/-} mice also suggests that changes in the photoreceptor terminals associated with rod-mediated light responses, including light-dependent changes of the calcium concentration at the synapse, do not contribute to the mechanisms underlying the phenotype of *Cabp4*^{-/-} mice. The light-independent phenotype corroborates the putative role of CaBP4 in photoreceptor synaptogenesis.

Electroretinograms were recorded to investigate the effect of CaBP4 deficiency on cone function. Single-flash ERG responses of the *Cabp4*^{-/-} *Gnat1*^{-/-} mice were severely reduced in scotopic conditions, whereas there was no significant difference in photopic conditions compared with *Cabp4*^{-/-} mice. Reduced-flicker ERG demonstrates that amplitudes and sensitivities of *Cabp4*^{-/-} *Gnat1*^{-/-} mice and *Cabp4*^{-/-} mice were significantly attenuated compared with those of *Gnat1*^{-/-} mice and wild-type mice, suggesting that few neural connections between cone cells and bipolar cells are functional in *Cabp4*^{-/-} and *Cabp4*^{-/-} *Gnat1*^{-/-} mice, in agreement with the results obtained using single-flash ERG recordings. These data demonstrate that in the absence of CaBP4, the synaptic transmission of the light response from cones to second-order neurons is severely affected. Unexpectedly, flicker ERG of *Gnat1*^{-/-} mice under scotopic and photopic conditions was attenuated compared with that of wild-type mice. This difference might be attributed to the different genetic backgrounds of wild-type mice and knockout mice.

Gresh et al.²¹ reported that a reduced amplitude of flicker ERG correlates with increasing flicker frequency more noticeably in Balb/c mice than in C57Bl/6 mice. To confirm the genetic background effects of mice for flicker ERG, double-heterozygous mice that comprise mixed C57BL/6, 129SvEv, and BALB/c backgrounds were prepared and analyzed with flicker ERG under the same conditions used in this study. However, no significant differences were observed between C57BL/6 wild-type mice and double-heterozygous mice (data not shown).

We have previously shown that CaBP4 interacts with expressed $\alpha 1F$ ($Ca_v1.4$) L-type, voltage-dependent calcium channels and modulates their functional properties.² Although the molecular identity of the cone Ca^{2+} channels is not fully elucidated, some cone channels contain the $Ca_v1.3$ sub-unit.²²⁻²⁴ Moreover, immunostaining of additional aggregates to typical horseshoe-shaped structures with an anti- $Ca_v1.4 \alpha 1F$ antibody suggests that $Ca_v1.4 \alpha 1F$ is also present in cone terminals.²⁵ The severely reduced cone signaling in CaBP4-deficient mice indicates that CaBP4 is also critical for the release of neurotransmitter from cone synaptic terminals. These results suggest that cones express the $Ca_v1.4$ subunit or a subunit highly homologous to it. The gene encoding the α -subunit of $Ca_v1.4$ appears to have diverged more recently from that of the human $Ca_v1.3$.²⁶ Their amino acid sequences share 70% overall similarity and 84% similarity between trans-membrane segments. Furthermore, in humans, mutations in the gene encoding the $Ca_v1.4 \alpha$ -subunit cause CSNB2. ERG responses of CSNB2 patients show reduced b-wave amplitude, but their color vision is almost, if not completely, normal, suggesting that cones express a calcium channel other than $Ca_v1.4$.

$Ca_v1.4$ -deficient mice also show ERG responses with an electronegative configuration and ectopic photoreceptor synapses (Orton NC, et al. *IOVS* 2004;45:ARVO Abstract 2507). $Cav1.4$ and $Cav1.3$ share biophysical properties; both activate at more negative voltages and more rapidly than $Cav1.2$, and both inactivate more slowly than $Cav1.2$. However, $Ca_v1.3 \alpha$ -deficient mice do not exhibit electroretinogram changes.²⁷ The phenotypes of CSNB2 patients and $Ca_v1.4$ -deficient and $Ca_v1.3$ -deficient mice can be reconciled if cones can be shown to coexpress two types of L-type voltage-dependent calcium channels. This would also be consistent with the critical role of CaBP4 in modulating rod and cone neurotransmitter release.

Acknowledgements

The authors thank Daniel Possin, supported by Vision Core Grant EY01730, for his great expertise with the EM experiments and Rebecca Birdsong for her help during manuscript preparation.

References

1. Haeseleer F, Sokal I, Verlinde C, et al. Five members of a novel Ca²⁺-binding protein (CABP) subfamily with similarity to calmodulin. *J Biol Chem* 2000;275:1247–1260. [PubMed: 10625670]
2. Haeseleer F, Imanishi Y, Maeda T, et al. Essential role of Ca²⁺-binding protein 4, a Ca(v)1.4 channel regulator, in photoreceptor synaptic function. *Nat Neurosci* 2004;7:1079–1087. [PubMed: 15452577]
3. Haeseleer F, Palczewski K. Calmodulin and Ca²⁺-binding proteins (CaBPs): variations on a theme. In: Baehr W, Palczewski K, eds. *Photoreceptors and Calcium* Vol. 514. Georgetown, TX: Landes Bioscience; 2002:303–317.
4. Haeseleer F, Imanishi Y, Sokal I, Filipek S, Palczewski K. Calcium-binding proteins: intracellular sensors from the calmodulin superfamily. *Biochem Biophys Res Comm* 2002;290:615–623. [PubMed: 11785943]
5. Sokal I, Li N, Verlinde C, Haeseleer F, Baehr W, Palczewski K. Ca²⁺-binding proteins in the retina: from discovery to etiology of human disease. *Biochim Biophys Acta Mol Cell Res* 2000;1498:233–251.
6. Lee A, Westenbroek RE, Haeseleer F, Palczewski K, Scheuer T, Catterall WA. Differential modulation of Ca(v)2.1 channels by calmodulin and Ca²⁺-binding protein 1. *Nat Neurosci* 2002;5:210–217. [PubMed: 11865310]
7. Zhou H, Kim SA, Kirk EA, et al. Ca²⁺-binding protein-1 facilitates and forms a postsynaptic complex with Ca(v)1.2 (L-Type) Ca²⁺ channels. *J Neurosci* 2004;24:4698–4708. [PubMed: 15140941]
8. Yang J, McBride S, Mak DOD, et al. Identification of a family of calcium sensors as protein ligands of inositol trisphosphate receptor Ca²⁺ release channels. *Proc Natl Acad Sci USA* 2002;99:7711–7716. [PubMed: 12032348]
9. Strom TM, Nyakatura G, Apfelstedt-Sylla E, et al. An L-type calcium-channel gene mutated in incomplete X-linked congenital stationary night blindness. *Nat Genet* 1998;19:260–263. [PubMed: 9662399]
10. Ball SL, Powers PA, Shin HS, Morgans CW, Peachey NS, Gregg RG. Role of the beta(2) subunit of voltage-dependent calcium channels in the retinal outer plexiform layer. *Invest Ophthalmol Vis Sci* 2002;43:1595–1603. [PubMed: 11980879]
11. Calvert PD, Krasnoperova NV, Lyubarsky AL, et al. Phototransduction in transgenic mice after targeted deletion of the rod transducin alpha-subunit. *Proc Natl Acad Sci USA* 2000;97:13913–13918. [PubMed: 11095744]
12. ChanLing T. Glial, vascular, and neuronal cytogenesis in whole-mounted cat retina. *Microsc Res Tech* 1997;36:1–16. [PubMed: 9031257]
13. Marc RE, Jones BW, Watt CB, Strettoi E. Neural remodeling in retinal degeneration. *Prog Retinal Eye Res* 2003;22:607–655.
14. Lyubarsky AL, Lem J, Chen J, Falsini B, Iannaccone A, Pugh EN. Functionally rodless mice: transgenic models for the investigation of cone function in retinal disease and therapy. *Vision Res* 2002;42:401–415. [PubMed: 11853756]
15. Goto Y, Yasuda T, Tobimatsu S, Kato M. 20-Hz flicker stimulus can isolate the cone function in rat retina. *Ophthalm Res* 1998;30:368–373.
16. Seeliger MW, Grimm C, Stahlberg F, et al. New views on RPE65 deficiency: the rod system is the source of vision in a mouse model of Leber congenital amaurosis. *Nat Genet* 2001;29:70–74. [PubMed: 11528395]
17. Peachey NS, Ball SL. Electrophysiological analysis of visual function in mutant mice. *Doc Ophthalmol* 2003;107:13–36. [PubMed: 12906119]
18. Humphries MM, Rancourt D, Farrar GJ, et al. Retinopathy induced in mice by targeted disruption of the rhodopsin gene. *Nat Genet* 1997;15:216–219. [PubMed: 9020854]
19. Lem J, Krasnoperova NV, Calvert PD, et al. Morphological, physiological, and biochemical changes in rhodopsin knockout mice. *Proc Natl Acad Sci USA* 1999;96:736–741. [PubMed: 9892703]

20. Claes E, Seeliger M, Michalakis S, Biel M, Humphries P, Haverkamp S. Morphological characterization of the retina of the CNGA3^{-/-}Rho^{-/-} mutant mouse lacking functional cones and rods. *Invest Ophthalmol Vis Sci* 2004;45:2039–2048. [PubMed: 15161873]
21. Gresh J, Goletz PW, Crouch RK, Rohrer B. Structure-function analysis of rods and cones in juvenile, adult, and aged C57BL/6 and Balb/c mice. *Vis Neurosci* 2003;20:211–220. [PubMed: 12916741]
22. Morgans CW, El Far O, Berntson A, Wassle H, Taylor WR. Calcium extrusion from mammalian photoreceptor terminals. *J Neurosci* 1998;18:2467–2474. [PubMed: 9502807]
23. Morgans CW. Calcium channel heterogeneity among cone photo-receptors in the tree shrew retina. *Eur J Neurosci* 1999;11:2989–2993. [PubMed: 10457194]
24. Barnes S, Kelly MEM. Calcium channels at the photoreceptor synapse. In: Baehr W, Palczewski K, eds. *Photoreceptors and Calcium* Vol. 514. Georgetown, TX: Landes Bioscience; 2002: 465– 476.
25. Morgans CW. Localization of the alpha(1F) calcium channel subunit in the rat retina. *Invest Ophthalmol Vis Sci* 2001;42:2414–2418. [PubMed: 11527958]
26. Bech-Hansen NT, Naylor MJ, Maybaum TA, et al. Loss-of-function mutations in a calcium-channel alpha(1)-subunit gene in Xp11.23 cause incomplete X-linked congenital stationary night blindness. *Nat Genet* 1998;19:264–267. [PubMed: 9662400]
27. Koschak A, Reimer D, Walter D, et al. Ca(v)1.4 alpha 1 subunits can form slowly inactivating dihydropyridine-sensitive L-type Ca²⁺ channels lacking Ca²⁺-dependent inactivation. *J Neurosci* 2003;23:6041– 6049. [PubMed: 12853422]

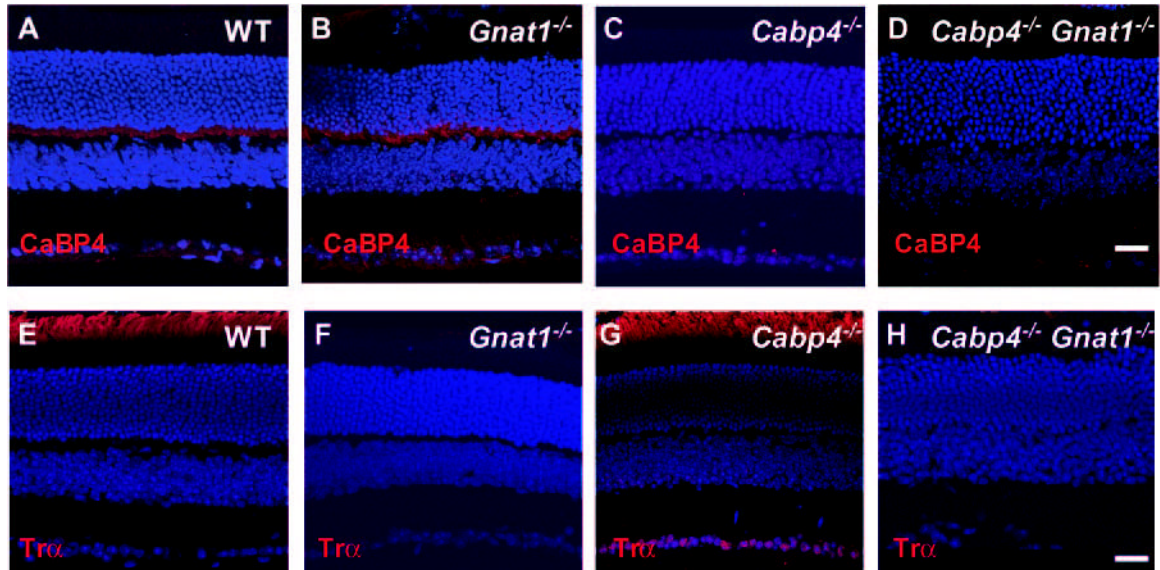


Figure 1.

Immunofluorescence staining of 2-month-old wild-type and knockout mice retina with antibodies recognizing CaBP4 and rod α -transducin. (A–D) Immunolocalization of CaBP4 (red). Labeling is observed in the outer plexiform layer. Some labeling is also observed in the inner segment. As expected, no CaBP4 immunoreactivity is detected in the retinas of *Cabp4*^{-/-} and *Cabp4*^{-/-} *Gnat1*^{-/-} mice. (E–H) Immunolocalization of rod α -transducin (red). Immunofluorescence is observed in the outer segment. No immunoreactivity is detected in the retina of *Gnat*^{-/-} and *Cabp4*^{-/-} *Gnat1*^{-/-} mice. (A–H) Nuclei are visualized by staining with Hoechst 33,342 dye. Scale bars, 20 μ m.

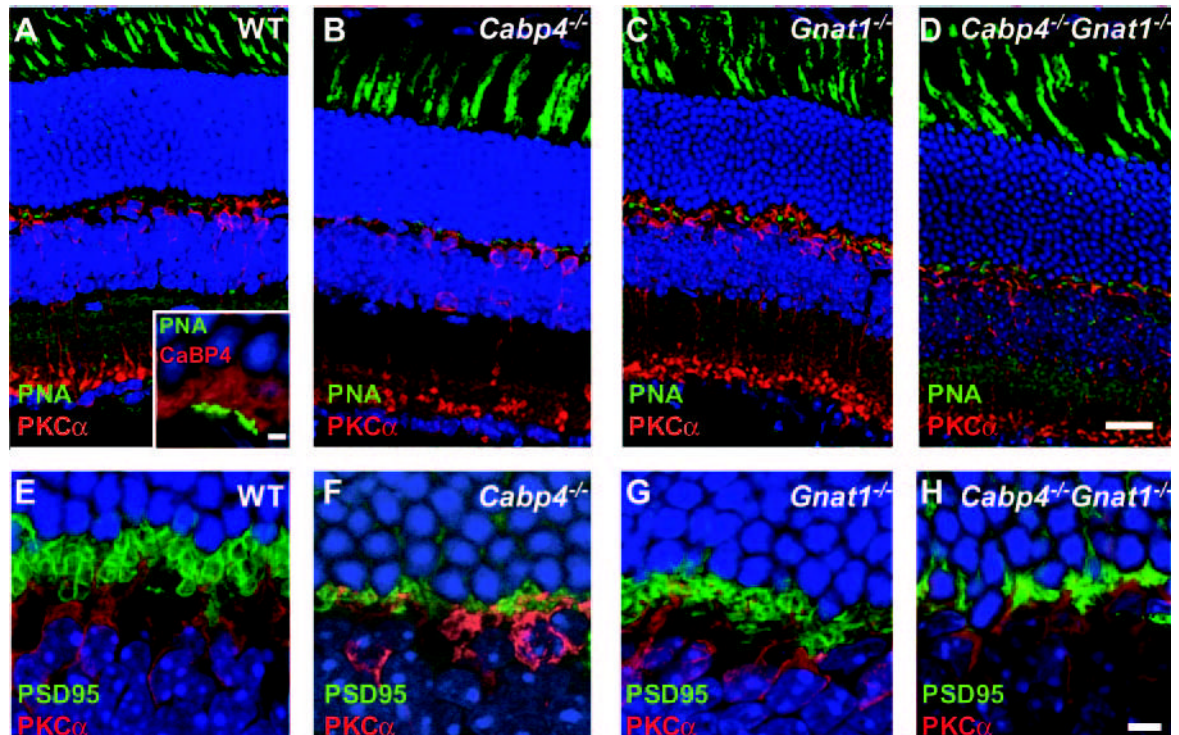


Figure 2.

Morphologic changes in the retinas of 2-month-old mice. (A–D) Immunolocalization of PKC α (red) and staining of cone photoreceptor with PNA (green). No difference was observed in the PNA staining pattern of cone photoreceptors between wild-type and single- and double-knockout mice. In wild-type mice, CaBP4 (red) is expressed in cones also labeled with PNA (green) (A, inset). CaBP4 staining is observed at the cone synaptic pedicles alongside the PNA-labeled synaptic membranes. CaBP4 staining is also observed in the rod spherules not labeled with PNA. (E–H) Synaptic changes in the OPL visualized by immunolocalization of PKC α (red) and PSD95 (green). Visualization of photoreceptor presynapses using anti-PSD95 antibody and of neuronal processes of rod bipolar cells using anti-PKC α . In wild-type and *Gnat1*^{-/-} mice, the photoreceptor terminals are inflated, whereas those in *Cabp4*^{-/-} and *Cabp4*^{-/-} *Gnat1*^{-/-} mice are disorganized and condensed. (A–H) Nuclei are visualized by staining with Hoechst 33,342 dye. Scale bars, (A–D) 20 μ m; (A, inset) 2 μ m; (E–H) 5 μ m.

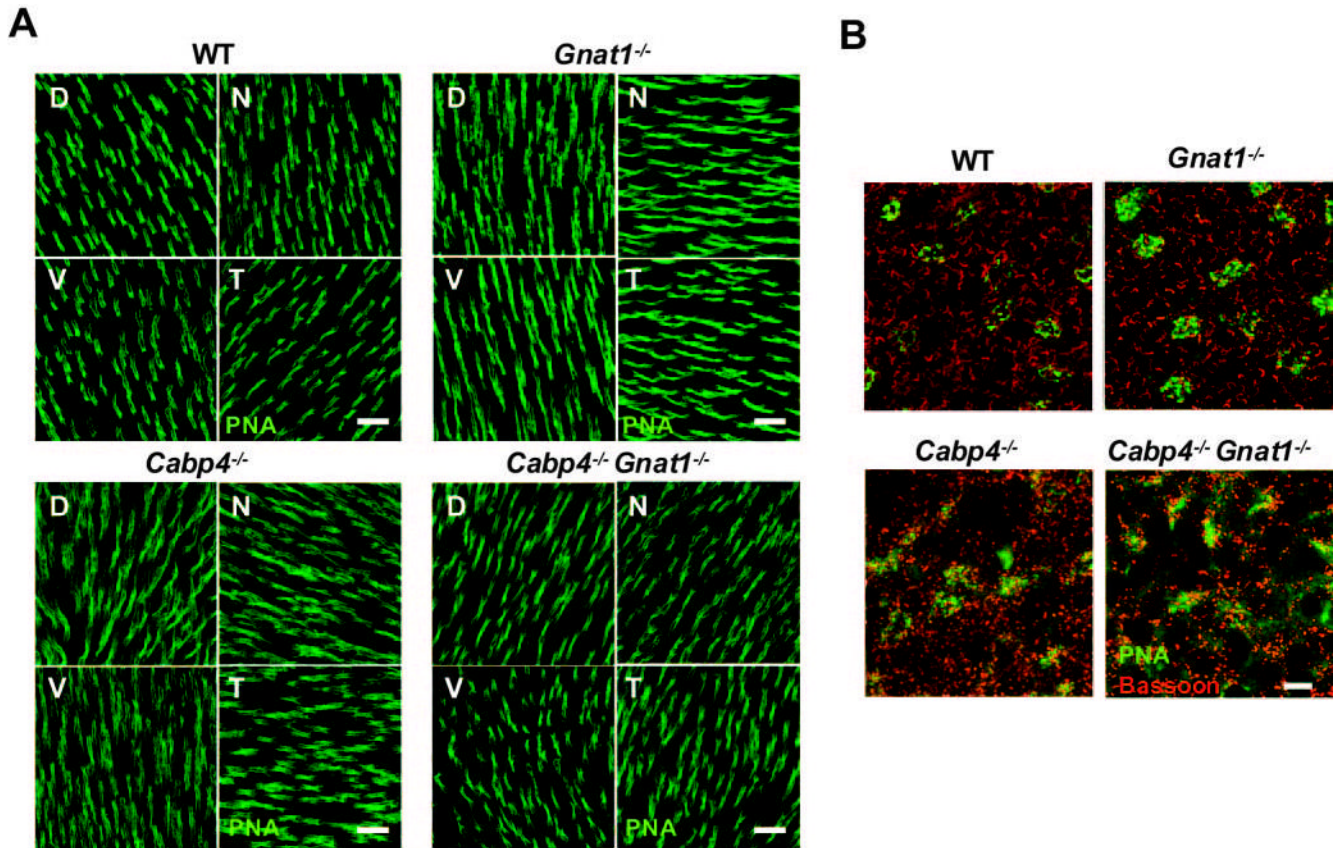


Figure 3.

PNA labeling of cones in retinal whole-mounts of 2-month-old mice. (A) Staining of cone outer segments in the four quadrants of flat-mounted retina labeled with PNA from wild-type and all knockout mice. D, dorsal; V, ventral; N, nasal, T, temporal. Scale bars, 20 μ m. (B) Double labeling with anti-bassoon (red) and PNA (green) across the outer plexiform layer in the temporal quadrant of the flat-mounted retina. Horseshoe-shaped structures are observed in wild-type and *Gnat1*^{-/-} mice, but mostly punctate staining is observed in *Cabp4*^{-/-} and *Cabp4*^{-/-} *Gnat1*^{-/-} mice. In wild-type and *Gnat1*^{-/-} mice, the PNA-labeled cone pedicles are round, but the cone pedicles of *Cabp4*^{-/-} and *Cabp4*^{-/-} *Gnat1*^{-/-} mice are more disorganized and appear spread out in a diamond-shaped structure. Scale bar, 5 μ m.

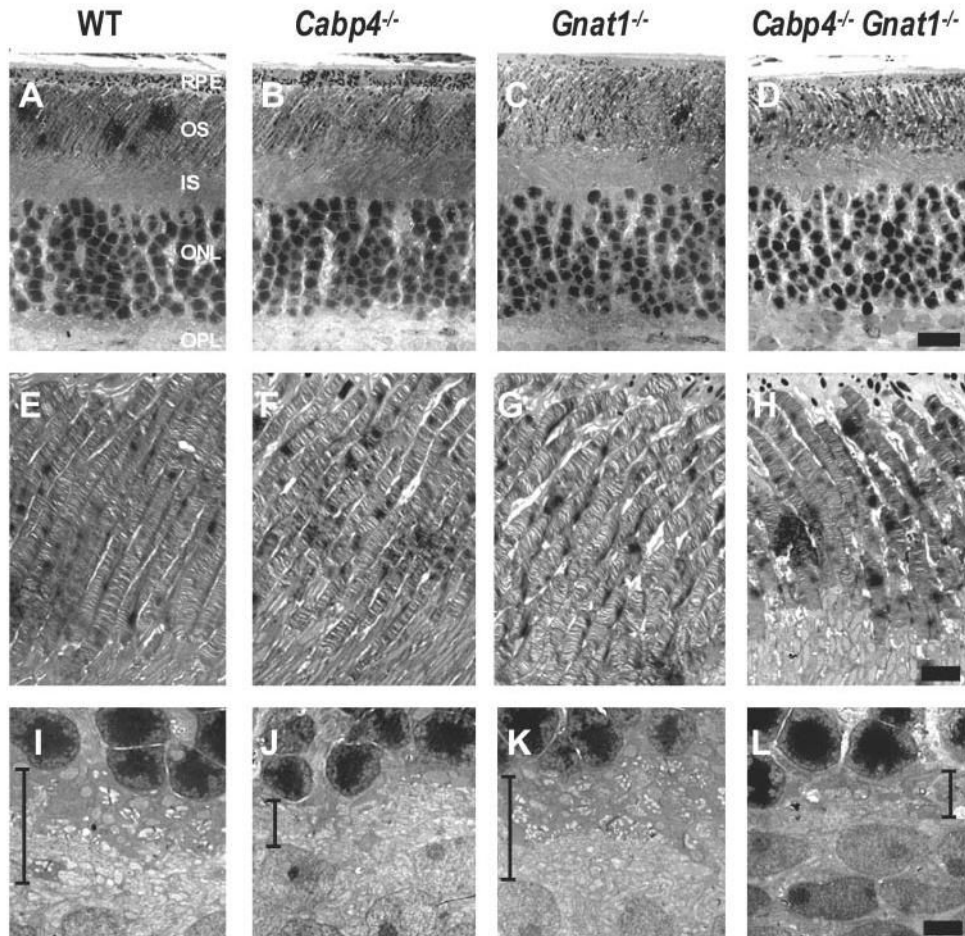


Figure 4.

Ultrastructure of photo-receptors of 2-month-old mice analyzed by transmission electron microscopy. (A–D) Cross-sections through the photoreceptors. The outer plexiform layer is thinner in *Cabp4*^{-/-} and *Cabp4*^{-/-} *Gnat1*^{-/-} mice than in wild-type mice. OS, outer segment; IS, inner segment; ONL, outer nuclear layer; OPL, outer plexiform layer. (E–H) Cross-sections through the OS. OS ultrastructure was comparable in retinas of knockout and wild-type mice (i.e., they were straight, parallel cylinders). (I–L) Cross-sections through the OPL. The OPL is delineated by *black lines*. Photoreceptor terminals that constitute the OPL in the wild-type and *Gnat1*^{-/-} mice were thinned in *Cabp4*^{-/-} and *Cabp4*^{-/-} *Gnat1*^{-/-} mice. Scale bars, (A–D) 10 μ m; (E–L) 2.5 μ m.

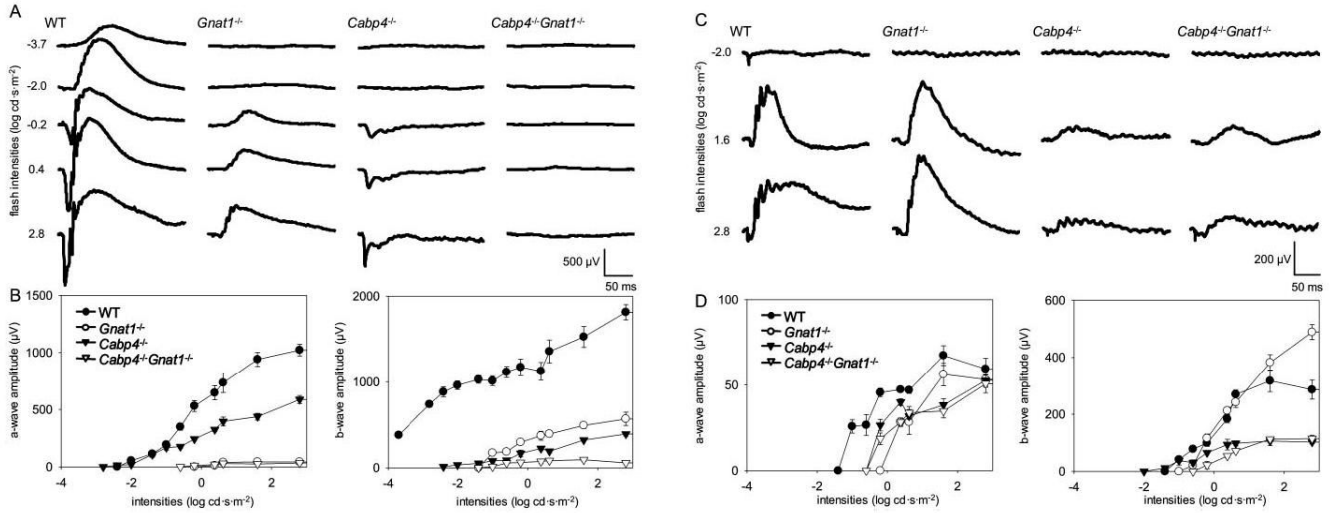


Figure 5. Single-flash ERG responses of increasing intensity for 2-month-old wild-type, *Gnat1*^{-/-}, *Cabp4*^{-/-}, and *Gnat1*^{-/-}*Cabp4*^{-/-} mice. Serial responses to increasing flash stimuli were obtained for wild-type, *Gnat1*^{-/-}, *Cabp4*^{-/-}, and *Gnat1*^{-/-}*Cabp4*^{-/-} mice for selected intensities under scotopic conditions (A) and photopic conditions (C) and were plotted as a function of a-wave and b-wave versus light intensity under scotopic conditions (B) and photopic conditions (D). In scotopic conditions, the a-wave amplitudes of *Gnat1*^{-/-}*Cabp4*^{-/-} mice were significantly reduced compared with those of wild-type and *Cabp4*^{-/-} mice ($P < 0.0001$), but they were not significantly reduced compared with those of *Gnat1*^{-/-} mice ($P > 0.1$). The b-wave amplitudes of *Gnat1*^{-/-}*Cabp4*^{-/-} mice in scotopic conditions were attenuated significantly compared with those of mice of all other genetic backgrounds ($P < 0.001$). In photopic conditions, the a-wave amplitudes of *Gnat1*^{-/-}, *Cabp4*^{-/-}, and *Gnat1*^{-/-}*Cabp4*^{-/-} mice were moderately reduced compared with those of wild-type mice ($P < 0.1$), whereas no significant differences were observed among those of *Gnat1*^{-/-}, *Cabp4*^{-/-}, and *Gnat1*^{-/-}*Cabp4*^{-/-} mice ($P > 0.1$). The b-wave amplitudes of *Cabp4*^{-/-} and *Cabp4*^{-/-}*Gnat1*^{-/-} mice were significantly attenuated ($P < 0.001$) compared with those of wild-type and *Gnat1*^{-/-} mice, whereas no significant difference was observed between those of *Cabp4*^{-/-} and *Gnat1*^{-/-}*Cabp4*^{-/-} mice. (B, D) SE bars are shown.

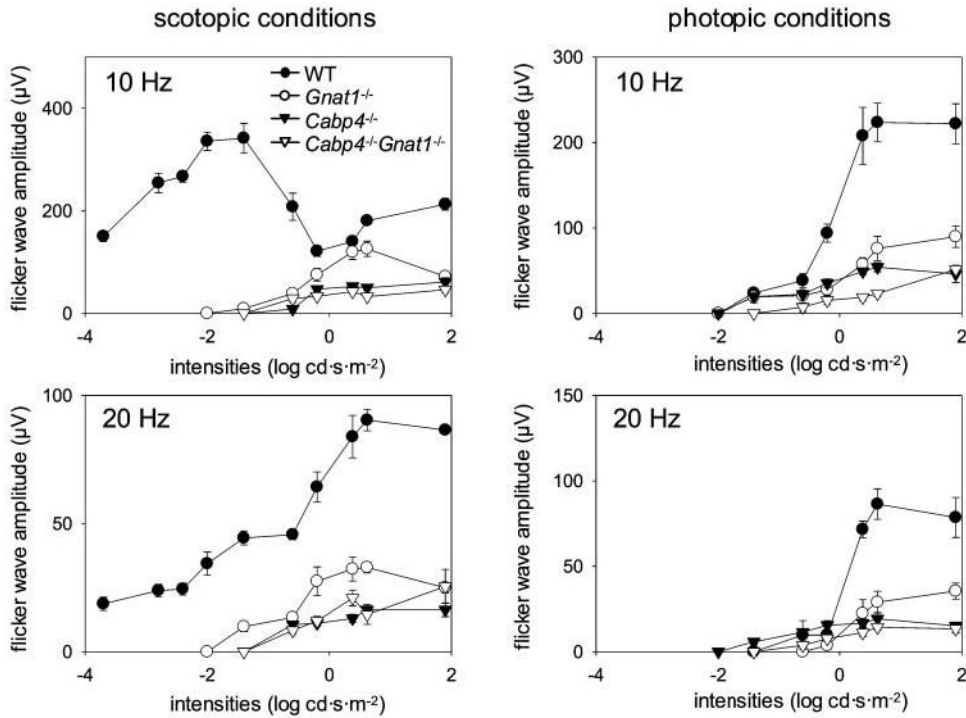


Figure 6.

Flicker-flash ERG responses of increasing intensity with various frequencies for wild-type, *Gnat1*^{-/-}, *Cabp4*^{-/-}, and *Gnat1*^{-/-}*Cabp4*^{-/-} mice. Flicker responses to increasing flash stimuli at varying frequency were obtained for wild-type, *Gnat1*^{-/-}, *Cabp4*^{-/-}, and *Gnat1*^{-/-}*Cabp4*^{-/-} mice and plotted as flicker wave amplitude versus light intensity under scotopic conditions (left) and photopic conditions (right). In scotopic conditions with 10- and 20-Hz stimulations, amplitudes and sensitivities of responses of *Gnat1*^{-/-}*Cabp4*^{-/-} mice and *Cabp4*^{-/-} mice were significantly attenuated compared with those of *Gnat1*^{-/-} and wild-type mice ($P < 0.001$), whereas no significant changes were observed between *Gnat1*^{-/-}*Cabp4*^{-/-} mice and *Cabp4*^{-/-} mice ($P > 0.1$). In photopic conditions with 10-Hz stimulation, *Gnat1*^{-/-}*Cabp4*^{-/-} mice showed significantly lower amplitudes and sensitivities than did other mice ($P < 0.01$). *Cabp4*^{-/-} mice revealed significantly reduced amplitudes compared with wild-type mice ($P < 0.0001$). Small changes, and these only at higher intensities ($P < 0.05$ at > 0.6 log cd · s · m⁻²), were observed in *Cabp4*^{-/-} mice compared with *Gnat1*^{-/-} mice. With 20-Hz stimulation, *Gnat1*^{-/-}*Cabp4*^{-/-} mice and *Cabp4*^{-/-} mice showed significantly attenuated responses compared with *Gnat1*^{-/-} and wild-type mice ($P < 0.001$), whereas no significant difference was observed between the attenuated responses of *Gnat1*^{-/-}*Cabp4*^{-/-} mice and *Cabp4*^{-/-} mice ($P > 0.1$). SE bars are shown.